

Experimental and Computational Verification of a New Remote Monitoring System Design for Spent Fuel Dry Cask Safeguards

Danielle M. South, Jeremy W. King, Sunil S. Chirayath, Craig M. Marianno

ABSTRACT

Spent nuclear fuel (SNF) is stored in dry casks following irradiation and initial cooling in spent fuel pools. Dry casks typically hold 2-6 dozen irradiated fuel assemblies. For a cask holding 32 assemblies, the mass of plutonium equates to around 20 significant quantities. Safeguard methods for dry cask storage currently rely on secure containment and constant surveillance. There is a need for increased security for dry casks to deter and detect the diversion of special nuclear material. A remote monitoring system (RMS) was designed to advance the current level of security and reliability of dry cask safeguards. The objectives of this study were to assess the performance of the external RMS as a diversion detection system and to develop a simulation approach for predicting neutron measurements for stable cask conditions as well as diversion scenarios. Small-scale neutron source experiments that mimicked SNF diversion from a dry storage cask were conducted and the non-detection probability was calculated for a variety of measurement times. MCNP simulations were carried out to assess the degree to which the measurement results could be predicted. The study concluded that the external RMS performs well as a neutron detection system and that MCNP simulation can be reliably used to predict measurements made by the RMS and non-detection probabilities in hypothetical diversion scenarios.

Keywords: Remote monitoring system, neutron detection, spent nuclear fuel, dry cask, continuity of knowledge, nuclear safeguards, non-detection probability, diversion

INTRODUCTION

Dry Casks are temporary spent fuel storage systems that are typically constructed of a steel canister and concrete overpack.² Casks hold SNF assemblies after they have been removed from a reactor and cooled for at least one year in a spent fuel pool to allow the decay of heat released from shorter lived fission products. A typical dry cask holds 32 pressurized water reactor (PWR) assemblies that altogether contain about 20 significant quantities (SQs) of plutonium.³ Current safeguards monitoring of these casks is limited to the continuity of knowledge (CoK) through containment and surveillance (C/S) methods such as seals and video monitoring.⁵ Currently, if CoK of a cask is lost, there is no method to verify the inventory of the cask except to relocate the cask to a pool, open it, and inspect the fuel. Procedures like this would be expensive, potentially dangerous, or totally infeasible if the cask is not on the same site as an available pool. An RMS that integrates C/S and non-destructive assay (NDA) through continuous radiation measurements is one solution to this problem. A successful PSM for dry cask safeguards would provide an additional way to maintain CoK in the event of a seal break or camera outage and verify the SNF content of a cask without having to open the cask.

Prior work done by researchers at Texas A&M University considered the utility of different types of RMSs as dry cask monitoring tools.⁶ Sagadevan studied the viability using fission chambers within dry casks as an RMS. The research simulated the internal RMS on a 32-assembly Holtec International Multi-Purpose Canister with HI-STORM overpack.^{7,8} While the simulation study found that the internal RMS could detect single fuel assembly diversions from a variety of fuel loadings, placing an RMS inside the cask drastically complicates routine maintenance and repairs

required for the system. Sagadevan then conducted a conceptual simulation study to take external measurements of the cask and concluded that the detection of SNF diversions from outside of the cask was feasible and further research should be conducted.

As a continuation of Sagadevan's work, researchers at TAMU designed and constructed an external RMS to further explore the feasibility of an external RMS. In this study, small-scale experiments with neutron sources mimicked SNF diversions from a spent fuel dry cask. These experiments assessed the performance of the new external RMS in detecting neutron source diversion for a variety of measurement durations. MCNP simulations corresponding to the experiments were also carried out to determine the degree to which the diversion measurements could be predicted. The objectives of this study were to assess the performance of the new external RMS as a detection system and to develop a simulation approach for predicting measurements.

METHODOLOGY

The external RMS design used in this study consisted of a 4 x 2 array of *Domino* neutron detectors. The detectors were encased in an ABS plastic shell and placed in a heavy-duty crate along with high density polyethylene (HDPE) above and below the detectors (Figure 1) to optimize neutron detection. The *Domino* detector was selected of this design because of its high neutron detection efficiency and its low cost commercial availability. The total cost of the RMS is about \$6,000.

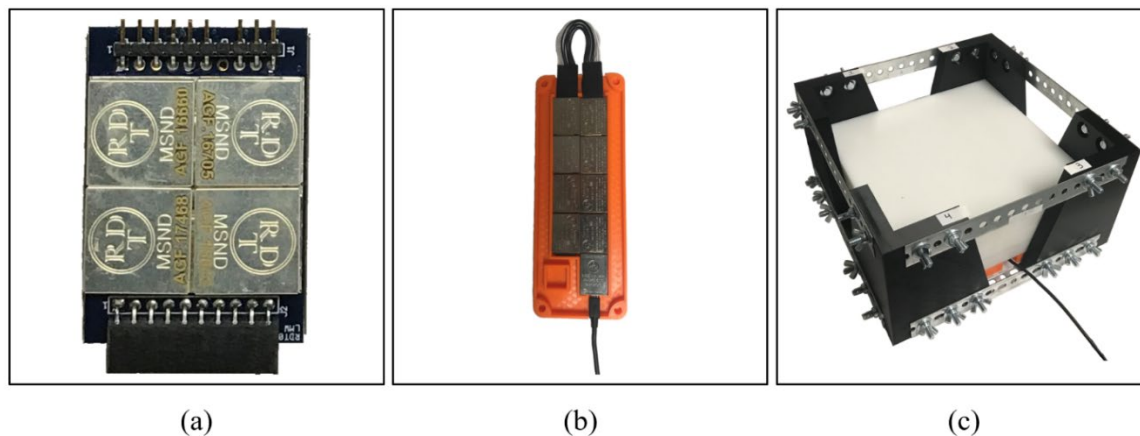


Figure 1. Photographs of (a) the *Domino* neutron detector, (b) the detector array and USB Driver Board, and (c) the external RMS

The *Domino* is a ${}^6\text{Li}$ -based semiconductor neutron detector developed by the Semiconductor Materials and Radiological Technologies (S.M.A.R.T.) Laboratory at Kansas State University and commercialized by Radiation Detection Technologies, Inc (RDT).^{9,10} The *Domino* is constructed of four *microstructured semiconductor neutron detector (MSND)* tiles. Deep etched trenches within the silicon diodes of the MSNDs are backfilled with 95% enriched ${}^6\text{LiF}$ to increase the probability of capturing alpha and triton particles emitted by the ${}^6\text{Li}(n,t){}^4\text{He}$ neutron capture reaction.^{9,11}

Small-scale experiments were conducted using five ${}^{252}\text{Cf}$ sources placed within a structure made of concrete and HDPE. The structure was arranged in a geometry that mimicked a one-eighth slice of a typical dry cask. The ${}^{252}\text{Cf}$ sources were placed on marked locations within the five areas of the cask structure (Figure 2). The placement of the sources and HDPE helped mimic the neutron

field produced by the volumetric signal of SNF assemblies in a spent fuel dry cask. The thickness of the HDPE within the RMS was optimized to provide the highest possible neutron count rate. The highest neutron count rate was achieved with 0.3175 cm of HDPE below the detector array, and 5.09 cm of HDPE above the detector array. This optimized configuration was used for the remainder of the study. Neutron count rates recorded in this study were five to six orders of magnitude lower than what would be recorded outside of a true dry cask. This means that implementation in a real SNF dry cask environment would result in better statistics and require less measurement time to reliably detect SNF diversion compared to the small-scale experiments in this study.

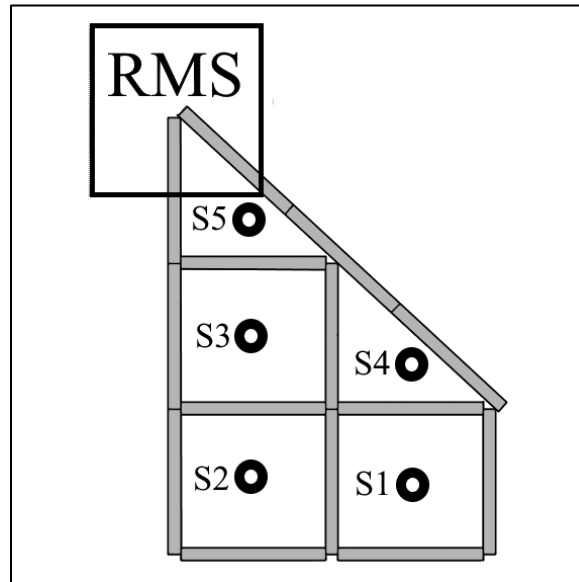


Figure 2. Diagram of small-scale experiment setup and source arrangement.

Measurements were conducted on the small-scale setup in seven source configurations and with five measurement durations for a total of 35 sample sets. The seven configurations were a neutron background measurement (BG), no sources diverted (ND), and diversion of each neutron source one-by-one (DS1 – DS5). The five real time measurement durations were: 15 s, 1 min, 5 min, 20 min, and 1 hr. The purpose of repeating measurements of the same configuration with different durations was to observe the effect of measurement time on the number of samples required to estimate the probability distribution of the neutron count rate as well as the calculated value of non-detection probability β .

The probability distribution of the neutron count rate for each sample set j was estimated as a normal distribution. To confirm the validity of the using a normal approximation on the samples sets, quantile plots were generated. Quantile plots are probability plots that compare the quantiles of sample sets to the quantiles of theoretical distributions.

For each measurement duration, the net neutron count rates, and standard deviations for ND and DS1 – DS5 were calculated by subtracting the BG count rate. Then, for a given false alarm probability, the alarm threshold was calculated from the net count rate and standard deviation of ND. Finally, the non-detection probability was calculated for each diversion scenario. These calculations are of relevance because in the application of nuclear safeguards monitoring, the null

hypothesis is that diversion has not occurred. A safeguards instrument classifies measurements as either a diversion (alarm) or no diversion (no alarm).

Simulations of the small-scale experiments were carried out using the Monte Carlo N-Particle radiation transport code, MCNP6.2. The purpose was to assess the degree to which measurements with the external RMS and calculated non-detection probabilities could be predicted by corresponding simulations. The output of the simulations was a pulse-height response of alpha and triton energy (MCNP F8:A,T tally) within the silicon of the *Domino* detectors. The MCNP simulations were performed until the tally achieved a relative stochastic error less than 0.1%.

RESULTS AND DISCUSSION

Measurements of the small-scale setup were taken in seven configurations (BG, ND, and DS1 – DS5) and for five measurement durations (15 s, 1 min, 5 min, 20 min, and 1 hr).

Table 1. Deadtime-corrected neutron count rate measurement data on top and standard deviation below in parenthesis [cps].

t (N)	Measured Count Rate, Mean // (Stdev.)						
	BG	ND	DS1	DS2	DS3	DS4	DS5
15 s (118)	0.40 (0.22)	9.21 (0.75)	8.59 (0.87)	7.48 (0.79)	5.30 (0.56)	8.88 (0.92)	6.92 (0.75)
1 min (29)	0.39 (0.08)	9.39 (0.38)	8.71 (0.38)	7.70 (0.33)	5.39 (0.22)	8.95 (0.33)	7.12 (0.37)
5 min (10)	0.33 (0.04)	9.55 (0.16)	8.75 (0.23)	7.93 (0.20)	5.34 (0.10)	9.11 (0.19)	7.20 (0.08)
20 min (1)	0.33 (0.02)	9.52 (0.09)	8.81 (0.09)	7.87 (0.08)	5.41 (0.07)	9.09 (0.09)	7.07 (0.08)
1 hr (1)	0.38 (0.01)	9.63 (0.05)	8.80 (0.05)	7.93 (0.05)	5.32 (0.04)	9.02 (0.05)	7.05 (0.04)

For each sample set of the 15 s, 1 min, and 5 min measurements, a Quantile-Quantile plot was produced.¹² The Quantile-Quantile plots for the 15 s, 1 min, and 5 min measurements of ND are provided in Figure 3. The plots demonstrate strong linear trends and contain few outliers. These features indicate that a normal distribution accurately represents the distribution of the data collected in the small-scale experiments.

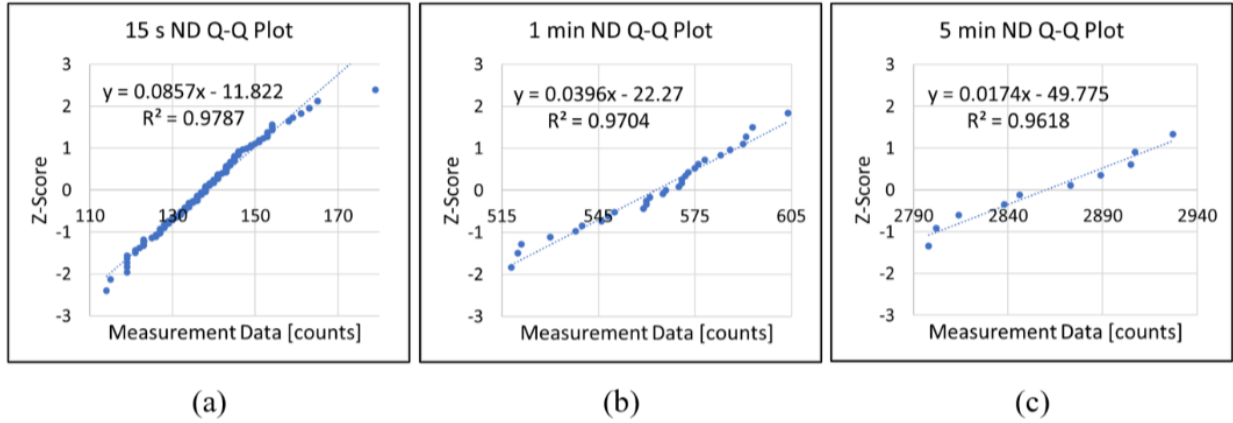


Figure 3. Quantile-Quantile plots for the 15 s, 1 min, and 5 min measurements of ND

For each measurement duration, the non-detection probability was calculated for all diversion scenarios with a false alarm probability = 5%. For safeguards monitoring, a false alarm probability of = 5% or lower is usually selected to minimize the operational burden of false alarms.⁴ A non-detection probability of $\beta = 10\%$ is enforced when a “high” probability of detection is desired, such as the diversion of an SQ of direct use material. Since there can be up to 20 SQs of plutonium within a single cask, only two fuel assemblies containing SNF would need to be diverted to acquire 1 SQ of plutonium. This is a situation in which a “high” detection probability is especially important. Table 2 displays the non-detection probabilities for all of the diversion scenarios and all measurement durations conducted in the study. The fourth diversion scenario (DS4) was the most challenging diversion to detect because of the weaker neutron signal of S4 due to its physical location relative to the RMS. The third diversion scenario (DS3) was the least challenging to detect due to its stronger neutron signal and being located closer to the RMS.

Table 2. Calculated non-detection probabilities β [%] for all measurements conducted in the study. All calculations were performed with a false-alarm probability $\alpha = 5\%$.

t	Non-detection Probability				
	DS1	DS2	DS3	DS4	DS5
15 s	77.4	29.6	< 0.1	84.5	10.1
1 min	45.6	0.1	< 0.1	72.1	< 0.1
5 min	1.1	< 0.1	< 0.1	18.9	< 0.1
20 min	< 0.1	< 0.1	< 0.1	0.1	< 0.1
1 hr	< 0.1	< 0.1	< 0.1	< 0.1	< 0.1

As measurement time for all of the experiment scenarios increased, the probability of non-detection gradually decreased. This trend is displayed in Figure 4. At the shortest measurement time (15 s), the normal distribution curves for ND and DS4 have significant overlap. This overlap results in a very large β . As measurement time increases, β decreases and eventually, with one hour of measurement time, the curves are adequately separated and β is nearly zero percent. In application, the measurement time should be chosen by the operators and regulator depending on the required β for the potential diversion scenario.

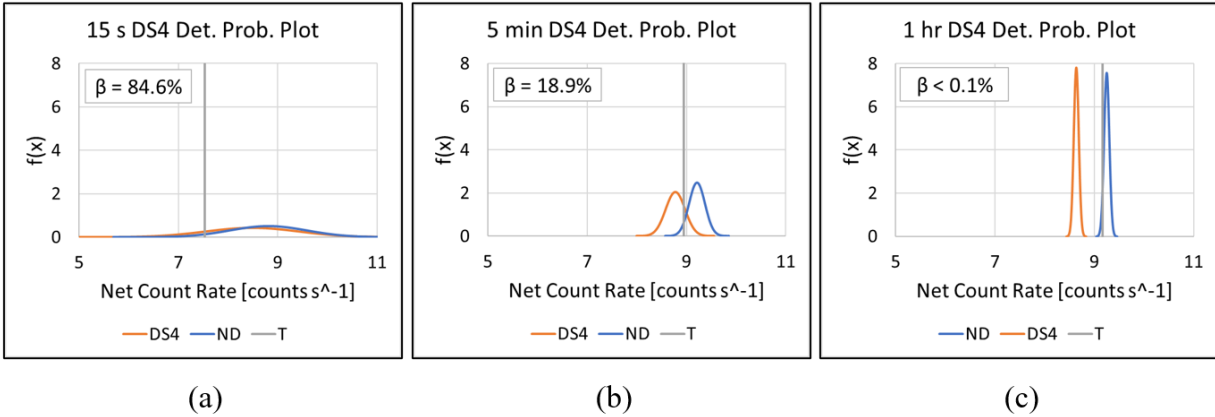


Figure 4. Detection probability plots of the curves for (a) 15 s, (b) 5 min, and (c) 1 hr measurements of DS4. As the measurement time increases, the value of β decreases.

The MCNP simulations overestimated the mean count rate of the non-diversion scenario and diversion scenarios 1-4, but underestimated diversion scenario 5. The reason for this bias is almost definitely the difference between the nominal source strengths and the unknown true source strengths. The implication of this bias is that the probability of non-detection for DS5 will always be lower than reality. This underestimation is of more concern than the overestimation because in scenarios like this, a more conservative approach to SNF diversion is desired. The non-detection probabilities calculated from both simulations and measurements in this study are tabulated in Table 3. The reported values are rounded to a single decimal place, so all non-detection probabilities below 0.05% are reported as “< 0.1%” for the measurement values and as “(0.0)” for the simulation intervals.

Table 3. Comparison of simulated interval and measured value of non-detection probability [%]

t	Non-detection probability, β [%], for $\alpha = 5\%$: MCNP // Meas.				
	DS1	DS2	DS3	DS4	DS5
15 s	[77.8, 83.9] 77.4	[24.6, 46.7] 29.6	(0.0, 0.0) 0.0	[85.2, 88.5] 84.5	[0.1, 3.7] 10.1
1 min	[42.6, 61.2] 45.6	[0.1, 2.7] 0.1	(0.0, 0.0) 0.0	[65.6, 76.8] 72.1	(0.0, 0.0) 0.0
5 min	[0.5, 7.1] 1.1	(0.0, 0.0) 0.0	(0.0, 0.0) 0.0	[11.4, 32.4] 18.9	(0.0, 0.0) 0.0
20 min	(0.0, 0.0) 0.0	(0.0, 0.0) 0.0	(0.0, 0.0) 0.0	(0.0, 0.5] 0.1	(0.0, 0.0) 0.0
1 hr	(0.0, 0.0) 0.0	(0.0, 0.0) 0.0	(0.0, 0.0) 0.0	(0.0, 0.0) 0.0	(0.0, 0.0) 0.0

Ultimately, the conducted MCNP simulations and the Monte Carlo approach for calculating β were successful in predicting the measured count rates and β s for generic diversion scenarios in a spent fuel dry cask system. This means that the MCNP simulation is a viable tool that can be used to estimate the non-detection probability of safeguards instruments.

CONCLUSION

Small-scale experiments using the designed external RMS detected ^{252}Cf neutron source diversions that mimicked SNF diversions from a dry cask. A statistical analysis concluded that if measurements times were sufficiently long, the data from the measurements could reasonably be analyzed as normally distributed. The non-detection probability β of each measured diversion scenario was calculated. It was observed that as measurement time increased, the non-detection probability β decreased. With 20 min measurements, the external RMS was able to detect all source diversions with non-detection probability $\beta \leq 10\%$. This value achieves the IAEA recommendation for high probability of detection which is especially important for high-risk scenarios involving as many significant quantities of plutonium as a typical dry cask contains. MCNP simulations were conducted which modeled each source and the simulations were performed to obtain results with very low stochastic error, and their results were combined to replicate the various measurement configurations. This study proved both the capability of the external RMS as a potential dry cask safeguards instrument and the utility of MCNP simulation in predicting the non-detection probability of diversion scenarios. The reliability of using MCNP for this application is particularly encouraging because it indicates the potential to study diversion scenarios, such as the removal of an SNF assembly from a dry cask, which would be expensive, logistically complex, and potentially dangerous to perform.

REFERENCES

1. J. King, C. Marianno, Experimental and Computational Verification of a New Remote Monitoring System Design for Spent Fuel Dry Cask Safeguards using Small-scale, Generic Diversion Scenarios
2. Nuclear Regulatory Commission, Dry Cask Storage, available at <https://www.nrc.gov/waste/spent-fuel-storage/dry-cask-storage.html> (accessed on December 15th, 2021).
3. A. Sagadevan, S. Chirayath, Information driven safeguards approach for remote monitoring system of dry cask storage, Nuclear Instruments and Methods in Physics Research, A, 954 (2020) 161737. <https://doi.org/10.1016/j.nima.2018.12.052> (accessed on December 15th, 2021).
4. IAEA Safeguards Glossary 2001 Edition, International Atomic Energy Agency, Vienna, 2003. <https://www.iaea.org/publications/6663/iaea-safeguards-glossary> (accessed on December 15th, 2021).
5. A. Fattah, N. Khlebnikov, International Safeguards Aspects of Spent-Fuel Disposal in Permanent Geological Repositories, International Atomic Energy Agency, 1990. <https://www.iaea.org/publications/magazines/bulletin/32-1/international-safeguards-aspects-spent-fuel-disposal-permanent-geological-repositories> (accessed on December 15th, 2021).

6. A.A. Sagadevan, Safeguards Approach for Spent Nuclear Fuel in Dry Cask Storage Using Remote Monitoring Systems, Texas A&M University, College Station, 2020. <https://hdl.handle.net/1969.1/192595> (accessed on December 15th, 2021).
7. A.A. Sagadevan, S.S. Chirayath, Design and analysis of an internal remote monitoring system for spent nuclear fuel stored in a dry cask, Nuclear Technology, (2021). <https://doi.org/10.1080/00295450.2021.1922259> (accessed on December 15th, 2021).
8. R. Kelly, P. Tsvetkov, S. Chirayath, J. Poston, E. Kitcher, Uncertainty Quantification of Concrete Utilized in Dry Cask Storage, Nuclear Technology, 190 (2015) 72–87. <https://doi.org/10.13182/NT13-155> (accessed on December 15th, 2021).
9. D.S. McGregor, W.J. McNeil, S.L. Bellinger, T.C. Unruh, J.K. Shultis, Microstructured semiconductor neutron detectors, Nuclear Instruments and Methods in Physics Research, A, 608 (2009) 125 – 131. <https://doi.org/10.1016/j.nima.2009.06.031> (accessed on December 15th, 2021).
10. S.L. Bellinger, W.J. McNeil, T.C. Unruh, D.S. McGregor, Characteristics of 3D Micro-Structured Semiconductor High Efficiency Neutron Detectors, IEEE Transactions on Nuclear Science 56 (2009) 742 – 746. <https://doi.org/10.1109/TNS.2008.2006682> (accessed on December 15th, 2021).
11. T.R. Ochs, Advanced dual-sided microstructured semiconductor neutron detectors and instrumentation, Kansas State University, Manhattan, 2020. <https://hdl.handle.net/2097/40545> (accessed on December 15th, 2021).
12. NIST/SEMATECH, Quantile-Quantile Plot, available at <https://www.itl.nist.gov/div898/handbook/eda/section3/qqplot.htm> (accessed on December 15th, 2021).